

# A Probabilistic Method for the Magnitude Estimation of a Historical Damaging Earthquake Using Structural Fragility Functions

by Hyeuk Ryu, Jae Kwan Kim, and Jack W. Baker

**Abstract** A method is proposed here to estimate the magnitude of a historical earthquake by using fragility functions and written descriptions of damage. Probabilistic descriptions are used to describe the distribution of potential earthquake events, the resulting intensity of ground shaking at the site, and the distribution of resulting damage to structures. This information is then combined using Bayes' theorem to compute the posterior distribution of the magnitude that caused a past damaging event. To validate the proposed method, the magnitude of the Northridge earthquake that occurred on 17 January 1994 is estimated. As an application example, the magnitude of a Korean earthquake that occurred in 1613 is estimated. Bins of input ground motions are created by a spectral matching method using an attenuation relationship of Korea, and probability-of-collapse estimates are obtained by performing incremental dynamic analysis (IDA). A basic formulation is presented and then extended to take the correlation of collapse capacity between structures, the effect of aging on structural response, and the site effects into account. Sensitivity analyses are performed to determine the importance of assumptions regarding the number of historically damaged buildings, the distributions of plausible magnitudes and distances, and the choice of attenuation relationship. The proposed method provides a comprehensive and straightforward procedure for magnitude estimation that can incorporate all relevant uncertainties.

## Introduction

In regions with low or moderate seismicity, such as Korea, most known destructive earthquakes occurred long before the advent of modern seismology and instrumentation. While these events play an important role in determining the level of design ground motion and in seismic hazard analysis, there is uncertainty as to their specific magnitude.

The most common and earliest approach for characterizing these events is to assign an intensity value, using a scale such as the Modified Mercalli Intensity (MMI), based on the damage described in historical documents. There are, however, two challenges associated with this approach: first, it lacks a standardized procedure for processing documentary data to perform intensity estimates (Castelli and Monachesi, 1996; Moroni *et al.*, 1996). Second, structural damage descriptions in an intensity scale are generally limited to a particular type of structure in a particular region (e.g., Japanese wooden houses in the Japan Meteorological Agency [JMA] seismic intensity scale), so it may not be valid for other types of structures in other regions.

Once the intensity of a historical earthquake is estimated, there are two ways to obtain its magnitude. One way is to use empirical relationships between magnitude and epicentral (maximum) intensity (Gutenberg and Richter,

1956; Topozada, 1975; Nuttli and Herrmann, 1978; Ambroseys, 1985). This is the only available method when a single damage description (data point) is available (Castelli and Monachesi, 1996). A second way is to use empirical relationships between magnitude and isoseismal area or radius (Muramatu, 1969; Topozada, 1975; Nuttli *et al.*, 1979; Ambroseys, 1985; Sibol *et al.*, 1987). The latter method has proved to be more reliable (less uncertain) than the former (Musson, 1996; Casado *et al.*, 2000), but both require instrumental data for the calibration or the construction of an empirical relationship, which is not possible in all regions of the world.

An alternative method is to estimate historical earthquake intensity through experimental and numerical studies of earthquake-damaged structures (Seo *et al.*, 1999; Choi and Seo, 2002; Kim and Ryu, 2003). Instead of using intensity scales that may not be suitable for all regions of the world, this method uses experimental structural testing and analysis to simulate structural damage described in historical documents; it then estimates ground-motion intensity using obtained relations between damage states and levels of input ground-motion intensity. This provides quantitative data for the estimation of historical ground-motion intensity,

although the data are dependent upon input ground motions and structural models.

As an extension of those previous experimental efforts, we propose a comprehensive probabilistic methodology for the magnitude estimation of historical earthquakes here. In the proposed method, structural damage due to a historical earthquake is modeled as a probabilistic event (termed damage event). The relationship between structural damage and ground-motion intensity is represented using a fragility function. Given the damage event and fragility function, the probability of the occurrence of the damage event given the ground-motion intensity, magnitude, and distance is computed. This is then combined with a relationship between ground-motion intensity and magnitude/distance (a ground-motion attenuation relationship) and a prior distribution of distance, applying the total probability theorem. This procedure computes the probability of the occurrence of the damage event given the magnitude. Ultimately, the posterior distribution of magnitude given the damage event is computed combining a prior distribution of magnitude and applying Bayes' theorem.

In this article, the proposed method is described in detail and validated by estimating the magnitude of the 1994 Northridge earthquake. As an application example, the magnitude of a historical Korean earthquake is then estimated. In addition, the proposed method is extended to take potential correlation of the collapse capacity between structures, the effect of aging on structural response, and the site effects into account. Sensitivity analyses are then performed to determine the importance of assumptions regarding the number of historically damaged buildings, the distributions of plausible magnitudes and distances, and the choice of attenuation relationship. The proposed method provides a comprehensive and straightforward procedure for magnitude estimation that can incorporate all relevant uncertainties.

## Methodology

A flow chart illustrating the proposed probabilistic method is shown in Figure 1. The main components of the procedure, highlighted in boldface for ease of reading, are explained in the following.

### Damage Event

Structural damage is usually qualitatively described in historic documents. However, we may transform a qualitative description of structural damage into a quantitative damage event if we assign a value for the number of structures in a specific damage state. Once the qualitative description is represented as a damage event, then its occurrence can be dealt with probabilistically.

As a simple case, a historical earthquake damage event, denoted  $E$ , can be defined as the collapse of  $n$  buildings out of  $n_t$  total buildings

$$E \equiv \{N = n\}, \quad 0 \leq n \leq n_t, \quad (1)$$

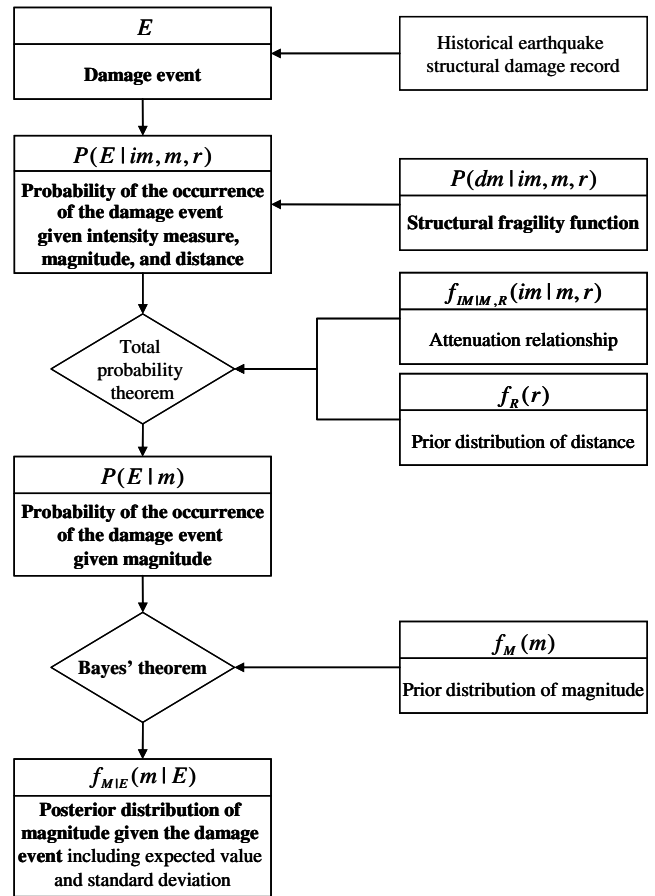


**Figure 1.** Flowchart of the probabilistic method for the magnitude estimation. (The main components of the procedure are shown in boldface type.)

where  $N$  is a random variable representing the number of collapsed structures,  $n$  is a specific numeric value of  $N$ , and  $n_t$  is total number of structures. Note that in the equations that follow, uppercase letters represent probabilistic events or random variables; lowercase letters represent numeric values.

Instead of assigning a single value for  $N$ , we may specify bounds for the number of collapsed structures such as

$$E \equiv \{l \leq N \leq u\} = \bigcup_{n=l}^u \{N = n\}, \quad 0 \leq l \leq n \leq u \leq n_t, \quad (2)$$

where  $l$  and  $u$  are lower and upper bounds on  $N$ , respectively, and  $\cup$  is the union symbol representing logical “or.”

Likewise, instead of considering a single damage state such as collapse in equation (1), we may define the event consisting of multiple damage states as

$$E \equiv \bigcap_{k=0}^{n_d} \{N_k = n_k\}, \quad 0 \leq n_k \leq n_t, \quad (3)$$

where  $k$  is the index for the damage state,  $n_d$  is the total number of damage states excluding nondamage state ( $k = 0$ ),  $\cap$  is the intersection symbol representing logical “and,”  $N_k$  is

the number of structures in the  $k$ th damage state, and  $n_k$  is a specific numeric value of  $N_k$ .

If we may assign bounds for the number of structures in multiple damage states, then the damage event can be represented as follows:

$$E \equiv \bigcup_{j=1}^{n_e} jE = \bigcup_{j=1}^{n_e} \left( \bigcap_{k=0}^{n_d} \{jN_k = jn_k\} \right), \quad 0 \leq jn_k \leq n_t, \quad (4)$$

where  $j$  is index for the subevents,  $n_e$  is the total number of subevents (or the width of bounds for the number of structures in any damage state),  $jE$  is the  $j$ th subevent consisting of single value for the number of structures in multiple damage states as represented by equation (3),  $jN_k$  is the number of structures in the  $k$ th damage state of the  $j$ th subevent, and  $jn_k$  is a specific numeric value of  $jN_k$ .

Furthermore, if we also consider multiple structural types, then the damage event can be represented as follows:

$$E \equiv \bigcap_{i=1}^{n_s} \left( \bigcup_{j=1}^{n_e^i} jE^i \right) = \bigcap_{i=1}^{n_s} \left[ \bigcup_{j=1}^{n_e^i} \left( \bigcap_{k=0}^{n_d} \{jN_k^i = jn_k^i\} \right) \right], \quad (5)$$

$$0 \leq jn_k^i \leq n_t^i,$$

where  $i$  is the index for the structure type,  $n_s$  is the total number of structure types,  $n_e^i$  and  $n_d^i$  are the total number of subevents and damage states of type  $i$  structure, respectively,  $jE^i$  is the  $j$ th subevent consisting of a single value for the number of type  $i$  structures in multiple damage states as represented by equation (4),  $jN_k^i$  is the number of type  $i$  structures in the  $k$ th damage state of the  $j$ th subevent,  $jn_k^i$  is a specific numeric value of  $jN_k^i$ , and  $n_t^i$  is the total number of type  $i$  structures.

The choice of equation that defines the damage event will depend upon the level of detail in the historical damage description.

### Structural Fragility Function

The structural fragility function represents the relationship between the structural damage state or the damage measure (DM) and the ground-motion intensity measure (IM); it is usually defined as a conditional probability of exceeding a damage state given a ground-motion intensity measure. The probability of equaling a damage state is thus calculated as follows:

$$P(\text{DM} = \text{dm}_k | \text{im}) = \begin{cases} 1 - P(\text{DM} \geq \text{dm}_1 | \text{im}) & k = 0 \\ P(\text{DM} \geq \text{dm}_k | \text{im}) - P(\text{DM} \geq \text{dm}_{k+1} | \text{im}) & 1 \leq k \leq n_d - 1 \\ P(\text{DM} \geq \text{dm}_{n_d} | \text{im}) & k = n_d \end{cases} \quad (6)$$

where  $\text{dm}_k$  is the  $k$ th damage state. If the damage states also depend on magnitude ( $M$ ) and distance ( $R$ ), then

$P(\text{DM} = \text{dm} | \text{im}, m, r)$  replaces  $P(\text{DM} = \text{dm} | \text{im})$  in equation (6). Fragility functions can be constructed based on expert opinions (e.g., Applied Technology Council (ATC-13) [1985]), empirically (e.g., Basoz and Kiremidjian [1997]), or analytically (e.g., Karim and Yamazaki [2001]). The analytical method is used in this study, as described later.

### Probability of the Occurrence of the Damage Event Given the IM, $M$ , and $R$

The probability of the occurrence of the damage event (i.e.,  $n$  collapses out of  $n_t$  structures) given a ground-motion intensity measure, magnitude, and distance can be computed using the multinomial distribution if we assume there is no correlation of building damage states between structures beyond that caused by the common ground-motion intensity.

For example, the probability of the occurrence of the damage event represented in equation (1), where a single value for the number of collapsed structure is assigned, can be computed using the binomial distribution, which is a special case of the multinomial distribution:

$$\begin{aligned} P(E | \text{IM} = \text{im}, M = m, R = r) &= P(N = n | \text{im}, m, r) \\ &= \frac{n_t!}{n!(n_t - n)!} \times P(\text{DM} = \text{collapse} | \text{im}, m, r)^n \\ &\quad \times P(\text{DM} = \text{noncollapse} | \text{im}, m, r)^{n_t - n}. \end{aligned} \quad (7)$$

The probability of the occurrence of the damage event represented in equation (2), which specifies bounds for the number of collapsed structure, can be computed using a summation of probabilities of events described by equation (1):

$$\begin{aligned} P(E | \text{IM} = \text{im}, M = m, R = r) &= P(l \leq N \leq u | \text{im}, m, r) \\ &= P \left[ \bigcup_{n=l}^u (N = n) \mid \text{im}, m, r \right] \\ &= \sum_{n=l}^u \frac{n_t!}{n!(n_t - n)!} \times P(\text{DM} = \text{collapse} | \text{im}, m, r)^n \\ &\quad \times P(\text{DM} = \text{noncollapse} | \text{im}, m, r)^{n_t - n}. \end{aligned} \quad (8)$$

The probability of the occurrence of the damage event represented in equation (3), which is composed of multiple damage states, is computed using the multinomial distribution:

$$\begin{aligned} P(E | \text{IM} = \text{im}, M = m, R = r) &= P \left[ \bigcap_{k=0}^{n_d} (N_k = n_k) \mid \text{im}, m, r \right] \\ &= \frac{n_t!}{\prod_{k=0}^{n_d} n_k!} \times \prod_{k=0}^{n_d} P(\text{DM} = \text{dm}_k | \text{im}, m, r)^{n_k}. \end{aligned} \quad (9)$$

Similarly, the probability of the occurrence of the damage event represented in equation (4), which is composed of bounds for the number of structures in multiple damage states, is computed as follows:

$$\begin{aligned}
P(E|IM = im, M = m, R = r) \\
&= P\left\{\bigcup_{j=1}^{n_e} \left[ \bigcap_{k=0}^{n_d} (jN_k = jn_k) \right] \middle| im, m, r \right\} \\
&= \sum_{j=1}^{n_e} \frac{n_t!}{\prod_{k=0}^{n_d} jn_k!} \times \prod_{k=0}^{n_d} P(\text{DM} = \text{dm}_k | im, m, r)^{jn_k}. \quad (10)
\end{aligned}$$

The probability of the occurrence of the damage event represented in equation (5), which is composed of bounds for the number of multiple types of structures in multiple damage states, is computed as follows:

$$\begin{aligned}
P(E|IM = im, M = m, R = r) \\
&= P\left( \bigcap_{i=1}^{n_s} \left\{ \bigcup_{j=1}^{n_e^i} \left[ \bigcap_{k=0}^{n_d^i} (jN_k^i = jn_k^i) \right] \right\} \middle| im, m, r \right) \\
&= \prod_{i=1}^{n_s} \left[ \sum_{j=1}^{n_e^i} \frac{n_t^i!}{\prod_{k=0}^{n_d^i} jn_k^i!} \times \prod_{k=0}^{n_d^i} P(\text{DM} = \text{dm}_k^i | im, m, r)^{jn_k^i} \right], \quad (11)
\end{aligned}$$

where  $\text{dm}_k^i$  is the  $k$ th damage state of type  $i$  structure.

#### Probability of the Occurrence of the Damage Event Given the $M$

Given the probability of the occurrence of the damage event given a ground-motion intensity measure, magnitude, and distance, the probability of the occurrence of the damage event given the magnitude is computed using  $f_{IM|M,R}(im|m, r)$ , which is a probability density function (PDF) of a ground-motion intensity given  $M$  and  $R$ , along with  $f_R(r)$ , which is a prior probability distribution of distance (i.e., a probability distribution of plausible distances of earthquakes) and applying the total probability theorem (Benjamin and Cornell, 1970)

$$\begin{aligned}
P(E|m) &= \iint P(E|im, m, r) \times f_{IM|M,R}(im|m, r) \\
&\quad \times f_R(r) \dim dr. \quad (12)
\end{aligned}$$

The probability density function of a ground-motion intensity given  $M$  and  $R$  can be obtained from attenuation relationships (e.g., Abrahamson and Silva [1997]), which relate IM with  $M$  and  $R$  and reflect the characteristics of ground motions of a specific region. The prior probability distribution of distance  $f_R(r)$  can be constructed based on subjective judgments, expert opinion, or previous research results on the estimation of epicenter locations.

#### Posterior Distribution of Magnitude Given the Damage Event

Given the probability of the occurrence of the damage event given the magnitude, the posterior distribution of magnitude given the damage event is computed by applying Bayes' theorem (Benjamin and Cornell, 1970 ),

$$\begin{aligned}
f_{M|E}(m|E) &= \frac{P(E|M = m) \times f_M(m)}{P(E)} \\
&= \frac{P(E|M = m) \times f_M(m)}{\int P(E|M = m) \times f_M(m) dm}, \quad (13)
\end{aligned}$$

where the prior probability distribution of magnitude  $f_M(m)$  can be constructed based on subjective judgments, expert opinions, or previous research results on the magnitude of the earthquake. It should be noted that the prior probability distribution is a description of plausible earthquake magnitudes; however, it does not yet take any information about the damage event into account (as that information will be incorporated in the other terms of equation 13). The conditional probability distribution of magnitude given the damage event is called the posterior probability distribution in the language of Bayesian probability. Using the posterior probability distribution of magnitude given the damage event, one can compute the expected value of magnitude given the damage event ( $\mu_{M|E}$ ) and standard deviation of magnitude given the damage event ( $\sigma_{M|E}$ ), respectively.

#### Validation Example

To validate the proposed method, we estimate the magnitude of the Northridge earthquake that occurred on 17 January 1994, as damage from that event is relatively well documented. Using precise instrumental data, the earthquake's moment magnitude was estimated as 6.7, and the epicenter was located about 2 km south-southwest of Northridge (34°12.53'N; 118°32.44'W) (Office of Emergency Services (OES), 1995). Using the damage data provided in Singhal and Kiremidjian (1998), we applied the proposed method to reestimate the magnitude of the Northridge earthquake.

#### Damage Event

The region studied by Singhal and Kiremidjian contained 184 low-rise ductile reinforced concrete (RC) frame buildings, four and six of which are identified as having minor (slight) and moderate damage, respectively, according to the relationship between the Park and Ang damage index (1985) and the damage state (Singhal and Kiremidjian, 1988). Thus, we assign numeric values for the number of structures in the damage states and define the damage event

$$E \equiv \{N_0 = 174\} \cap \{N_1 = 4\} \cap \{N_2 = 6\}, \quad n_t = 184, \quad (14)$$

where subscripts 0, 1, and 2 represent the damage states of none, slight, and moderate, respectively.

### Structural Fragility Function

To determine fragility functions for this example, we adopt the equivalent-PGA (peak ground acceleration) fragility functions presented in HAZUS methodology (Federal Emergency Management Agency [FEMA], 2003). These fragility functions are defined with two parameters as

$$P(\text{DS} \geq \text{ds} | \text{PGA} = x) = \Phi\left(\frac{\ln x - \ln \overline{\text{PGA}}_{\text{ds}}}{\beta_{\text{SPGA}}}\right), \quad (15)$$

where  $\overline{\text{PGA}}_{\text{ds}}$  represents the median PGA of structural damage state, ds, and  $\beta_{\text{SPGA}}$  quantifies the variability of PGA values that may cause exceedance of the damage state. The median PGA of the structural damage state is computed using the spectrum shape ratio of demand spectrum and the soil amplification factor. Here the spectrum shape ratio is computed by linear interpolation of the values provided in the HAZUS technical manual. For example, the spectrum shape ratio at magnitude 5.5 is computed as 2.55 by interpolating 3.3 and 1.8, which are the values at magnitudes 5 and 6, respectively. Also, the soil amplification factor is set to 1, and  $\beta_{\text{SPGA}}$  is set to 0.64 as provided in the HAZUS technical manual (FEMA, 2003). Given the computed equivalent-PGA fragility functions, we compute the probability of equaling a damage state using equation (6).

### Probability of the Occurrence of the Damage Event Given the IM, $M$ , and $R$ and Probability of the Occurrence of the Damage Event Given the $M$

The probability of the occurrence of the damage event given the PGA,  $M$ , and  $R$  is computed using equation (9), which can be represented as

$$\begin{aligned} P(E | \text{PGA} = x, M = m, R = r) &= \frac{184!}{174! \times 4! \times 6!} \times P(\text{DM} = \text{none} | x, m, r)^{174} \\ &\times P(\text{DM} = \text{slight} | x, m, r)^4 \\ &\times P(\text{DM} = \text{moderate} | x, m, r)^6. \end{aligned} \quad (16)$$

To compute the probability of the occurrence of the damage event given the magnitude, we used the Abrahamson and Silva (1997) attenuation relationship for  $f_{\text{IM}|M,R}(\text{im}|m, r)$ , reflecting the characteristics of ground motions in the western United States. For this simple validation, the distance from the epicenter to the damaged building area is assumed constant for all buildings and is set equal to 20 km, as the damaged buildings were located between 5 and 30 km from the epicenter. We compute the probability of occurrence of the damage event given the magnitude using equation (12). Figure 2 shows the probability of the occurrence of the damage event given the magnitude and shows

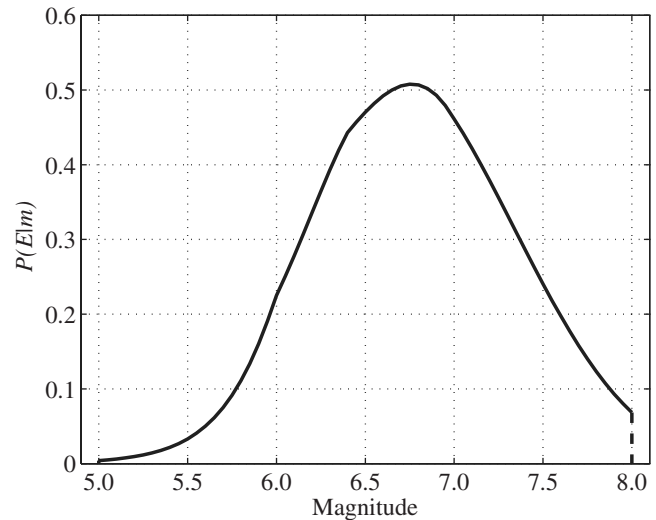


**Figure 2.** Probability of the occurrence of the damage event given the magnitude.

that an earthquake event of  $M$  6.8 has the highest probability of causing the given damage event.

### Posterior Distribution of Magnitude Given the Damage Event

In this example, we choose a uniform distribution of magnitude

$$f_M^1(m) = \frac{1}{m_u - m_l}, \quad m_l \leq m \leq m_u, \quad (17)$$

where  $m_l$  and  $m_u$  are the lower and upper limits of magnitude, respectively, and are set equal to 5 and 8, reflecting the range of magnitudes that is believed to be feasible in the western United States and could damage structures. Note that a superscript 1 is added to distinguish this from alternative magnitude distributions used later in the application example.

We compute the posterior probability distribution of magnitude given the damage event using equation (13). Figure 3 shows the prior distribution of magnitude, as well as the posterior distribution given the damage event. The expected value and standard deviation from the posterior magnitude distribution are approximately 6.8 and 0.5, respectively. With alternative values of the distance from 10 to 30 km, the expected values ranged from 6.4 to 7.0, while the standard deviations always fell in the range between 0.5 and 0.6.

### Discussion of Validation Result

The aforementioned obtained estimated magnitude values are consistent with the known true magnitude of 6.7 for this event. It should be noted that the fragility functions developed in the HAZUS methodology were compared and verified with previous earthquakes including the Northridge earthquake (Kircher *et al.*, 1997). Thus, the validation

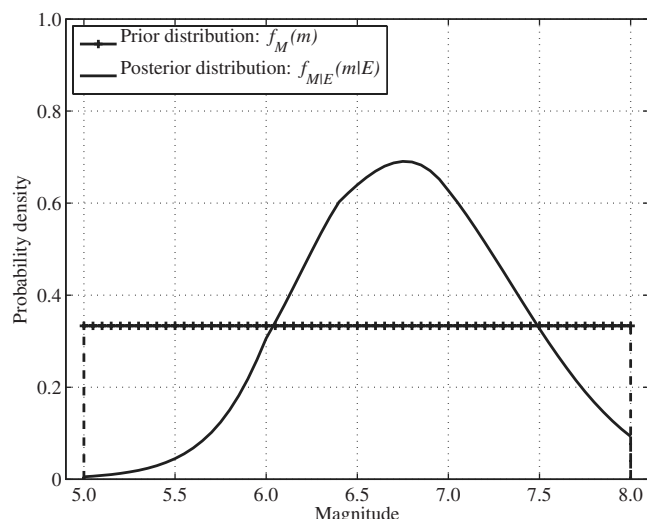


**Figure 3.** Posterior probability distribution of magnitude given the damage event with prior distribution of magnitude.

may be somewhat circular as it relies on fragility functions based in part on the data used in this calculation. Nonetheless, the results appear to demonstrate that the proposed methodology will produce reasonable magnitude estimates, at least in the case where reasonable fragility functions are used in the analysis.

### Application Example

As an application example, the magnitude of a Korean earthquake that occurred in 1613 is estimated. Structural damage due to the 1613 earthquake was recorded in the Annals of the Choson Dynasty. Previous researchers have estimated the epicentral (maximum) intensity as 6–8 on the MMI scale and its magnitude as 5.3–6.5 on the Richter magnitude scale, as summarized in Table 1.

The epicenter has been estimated to have been in Seoul, the capital of the Choson Dynasty (Korea Ministry of Construction and Transportation [KMOCT], 1997; Lee, 1998; Chu and Lee, 1999; Seoul Development Institute [SDI], 1999). This example calculation is performed to demonstrate the proposed method rather than to give an exact estimate of the earthquake’s magnitude.

**Table 1**  
Previous Estimations on the 1613 Earthquake

Source	Magnitude	MMI
Li, 1986	6.5	N/A
KMOCT, 1997	N/A	6
Lee, 1998	N/A	7
SDI, 1999	5.8	8
Chu and Lee, 1999	5.5	7

### Damage Event

A historic document describing the earthquake damage indicated that many houses collapsed (see Fig. 4). The text does not describe the type of house, but it is widely recognized that wooden houses with thatched and tiled roofs were the most common types of structures at that time. Experts on Korean history and the history of Korean architecture recommend that the collapsed houses be classified as wooden houses with thatched roofs (B. H. Jeon, personal comm., 2000; S. D. Huh, personal comm., 2005). The damage state recorded in the historic document is collapse, so we use equation (2) to define the damage event in terms of collapses and noncollapses. The total number of buildings is estimated to be 4500 based on historical census data (Kyujeonggak Institute for Korea Studies at Seoul National University, 1996) and information on the portion of wooden houses with thatched roofs (Kim, 1994). The lower and upper estimates of the number of collapse building are initially estimated as 20 and 45, respectively, and later, sensitivity studies will be performed to examine the importance of this assumption.

### Structural Fragility Function

To compute the probability of collapse of a house, a calibrated numerical model for wooden houses with thatched



**Figure 4.** Image of earthquake damage record. The English translation of the record is as follows: “The earthquake occurred at dawn. It sounded like it was very loud thunder and many houses collapsed” (see Data and Resources section).

roofs is developed and then subjected to a series of ground motions. A two-dimensional portal frame consisting of beam, column, and nonlinear rotational springs is used to model a typical house (Fig. 5). The natural period of model is set to be 0.6 sec (1.67 Hz), and the damping ratio is set to be 10%, based on the shaking table test results of Korean traditional wooden houses (Seo *et al.*, 1999; Ryu *et al.*, 2006).

To simulate nonlinear behavior observed in static tests of portal frames (Ryu *et al.*, 2006), nonlinear rotational springs between the beams and columns were used. The spring has a backbone curve with a negative slope after a capping point, which is capable of simulating collapse of the model (Ibarra, 2003). It also has a pinching hysteresis with cyclic deterioration (Ibarra, 2003) that was observed in a cyclic loading test of an experimental frame (Ryu *et al.*, 2006).

The backbone curve and pinching hysteresis of the nonlinear rotational spring is depicted in Figure 6. Note that the ratio of  $\theta_c$  and  $\theta_y$  (so-called ductility) is significantly larger than that of typical modern buildings, as  $\theta_y$  is not a true yielding point but is rather selected to match experimental results. The yielding point in this structure occurs when there is a loss of contact forces at some points in the beam-column connection, and the structure is able to undergo significant further displacement before reaching the negative-stiffness portion of the backbone curve. All hysteresis model parameters except negative capping stiffness, which is equal to  $-0.02$ , are calibrated based on cyclic loading test results (Ryu *et al.*, 2006). Parameter values of  $\kappa_d$  and  $\kappa_f$  of the pinching model are set to 0.3 and 0.7, respectively, and all values of parameters of cyclic deterioration model are set to 500.

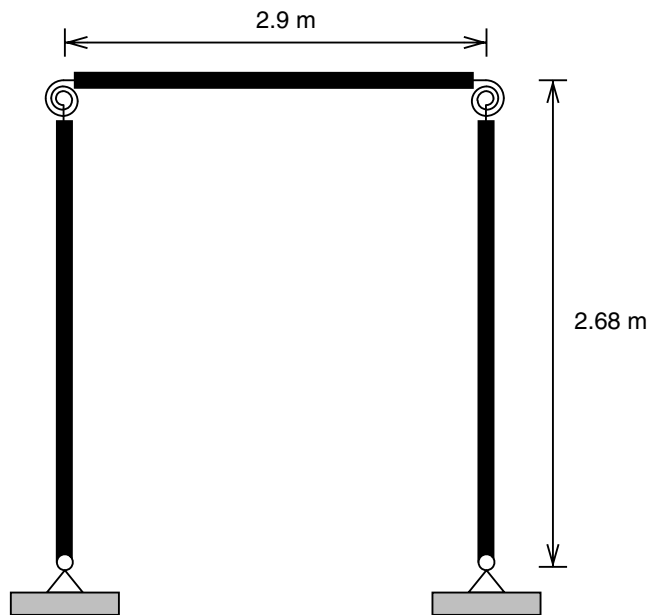


**Figure 5.** Two-dimensional portal frame for numerical simulations.

No earthquakes with  $M > 6.5$  were recorded in Korea, so we take ground motions recorded in active seismic regions and modify them to reflect the differences in the expected frequency content of Korean ground motions. The procedure presented in NUREG/CR-6728 (McGuire *et al.*, 2001) is used to develop these ground motions. This procedure creates hybrid empirical records that maintain realistic phase and amplitude relationships between components and realistic frequency-to-frequency variability through a weak spectral matching process implemented in the code RASCAL (Silva and Lee, 1987). The KEPRI01 attenuation relationship (Korea Institute of Nuclear Safety [KINS], 2003) is used to compute target spectra for this study because it is the only Korean attenuation relationship that provides median and standard deviation of spectral acceleration given magnitude and distance. Figure 7 shows the median spectral accelerations predicted by the KEPRI01 (KINS, 2003) and Abrahamson and Silva (1997) attenuation relationships. This shows how the amplitude and relative frequency content of ground motions varies between Korea and the active seismic regions for which the Abrahamson and Silva (1997) model was developed.

We select five bins of input ground motions, representing various magnitude and distance ranges: (1)  $5 \leq M \leq 6$ ,  $0 \leq R \leq 50$ , (2)  $6 \leq M \leq 7$ ,  $0 \leq R \leq 10$ , (3)  $6 \leq M \leq 7$ ,  $10 \leq R \leq 50$ , (4)  $7 \leq M \leq 8$ ,  $10 \leq R \leq 50$ , and (5)  $7 \leq M \leq 8$ ,  $50 \leq R \leq 100$ . Using a database of western United States records from the NUREG/CR-6728 report (McGuire *et al.*, 2001), the NUREG procedure is used to create 15 ground motions for each magnitude-distance bin (except for the  $6 \leq M \leq 7$ ,  $10 \leq R \leq 50$ , which has 30 ground motions). Note that numbers of ground motions are based on the number of records provided in the NUREG database. All ground motions have two horizontal components for a total of 180 time history components. Figure 8 shows the time histories of acceleration, velocity, and displacement of recorded ground motion from the 1971 San Fernando earthquake ( $M$  6.6,  $R = 24.2$  km) and those of corresponding modified ground motion.

For the construction of the collapse fragility function, incremental dynamic analyses (Vamvatsikos and Cornell, 2002) are performed using the Pacific Earthquake Engineering Research (PEER) Center's OpenSees platform (McKenna and Fenves, 2001) to get a distribution of collapse capacities. Spectral acceleration at the fundamental period of a numerical model with a damping ratio of 5% is chosen as the ground-motion intensity measure. Collapse is assumed to occur when the drift ratio (the ratio of horizontal displacement to the height of the structure) reaches 0.15.

If the distribution of collapse capacity is assumed to be lognormal, then the collapse fragility function is

$$P(\text{collapse} | S_a = x) = P(S_{a,c} \leq x) = \Phi\left(\frac{\ln x - \hat{\lambda}}{\hat{\zeta}}\right), \quad (18)$$

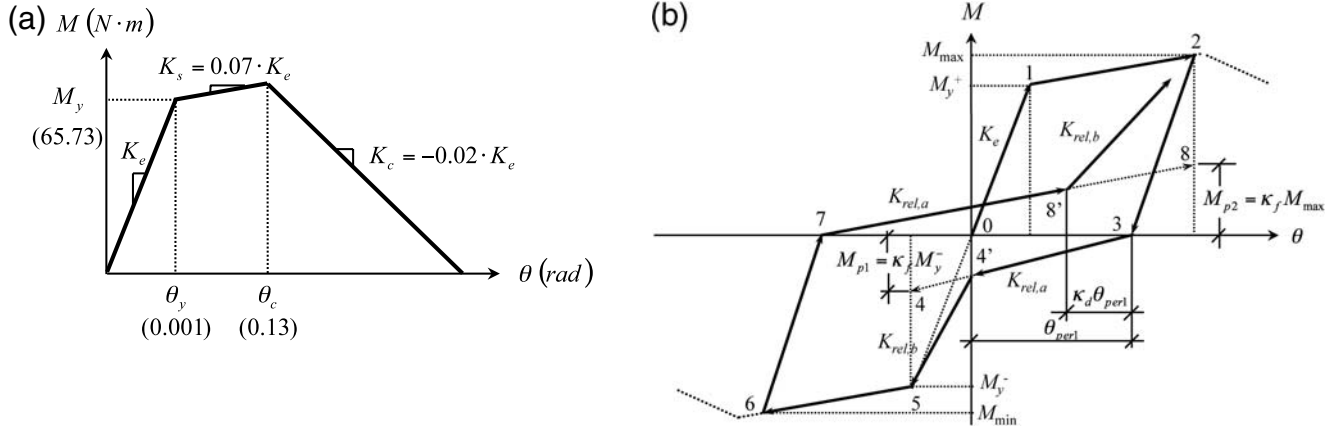


**Figure 6.** Hysteresis model of a nonlinear spring between the beam and column (adapted from Ibarra [2003]). (a) Backbone curve relating the moment in the joint ( $M$ ) to the joint rotation ( $\theta$ ) (not to scale). (b) Pinching hysteresis model.

where  $S_a$  represents  $S_a(T_1 = 0.6 \text{ sec})$ ,  $S_{a,c}$  represents the  $S_a(T_1 = 0.6 \text{ sec})$  at collapse,  $\hat{\lambda}$  and  $\hat{\zeta}$  are the estimated mean and standard deviation, respectively, of logarithmic collapse capacity, and  $\Phi$  is the standard normal cumulative distribution function.

Figure 9 shows the incremental dynamic analysis (IDA) curves for the  $5 \leq M \leq 6$ ,  $0 \leq R \leq 50$  and  $7 \leq M \leq 8$ ,  $50 \leq R \leq 100$  bins. The difference between these two suggests that collapse capacity is affected by the ground motions' magnitude and/or distance values. We also consider the epsilon ( $\epsilon$ ) as a possible predictor of collapse capacity, as it can

account for the effect of spectral shape on the collapse capacity (Baker and Cornell, 2006). The value of the epsilon for a given ground motion and period is calculated as

$$\epsilon = \frac{\ln(S_a) - \hat{\mu}_{\ln S_a}}{\hat{\sigma}_{\ln S_a}}, \quad (19)$$

where  $\hat{\mu}_{\ln S_a}$  and  $\hat{\sigma}_{\ln S_a}$  are the mean and standard deviation, respectively, of logarithmic spectral acceleration, as predicted by the attenuation equation.

Figure 10 shows the relationships between collapse capacity and magnitude and epsilon, respectively. The ob-

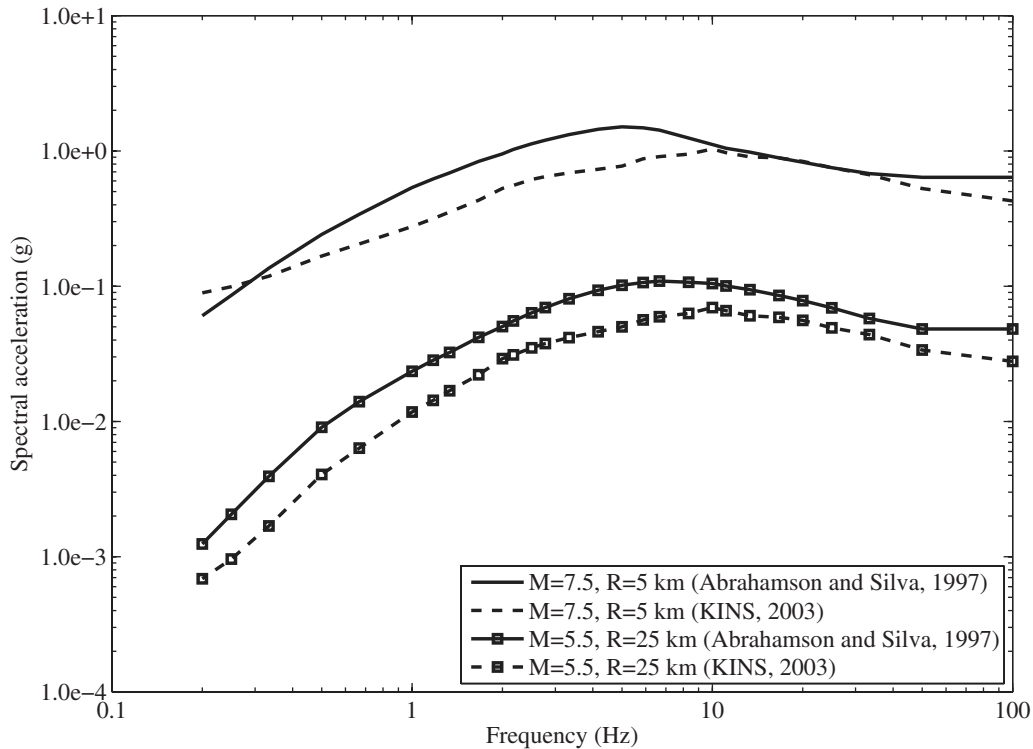


**Figure 7.** Median spectral acceleration predicted by KEPRI01 (KINS, 2003) for Korea and that predicted by Abrahamson and Silva (1997) for active shallow crustal seismic regions.

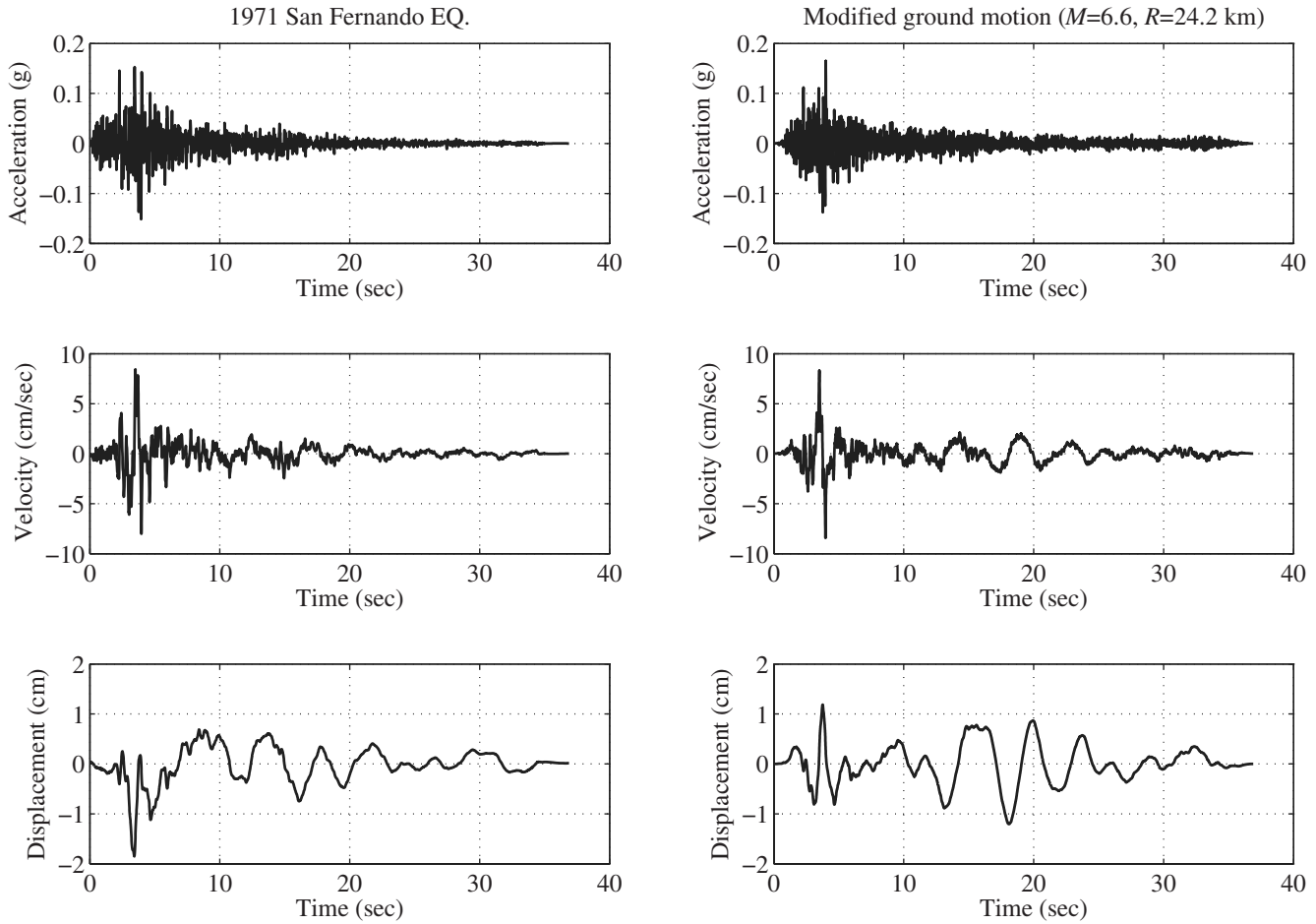


**Figure 8.** Time histories of acceleration, velocity, and displacement of the 1971 San Fernando earthquake (Lake Hughes #4 recording) and the corresponding modified ground motion.

served strong correlation between collapse capacity and magnitude is notable, given that previous researchers have not observed strong magnitude dependence in response results (e.g., Bazzurro and Cornell [1994], Shome *et al.* [1998], and Iervolino and Cornell [2005]). It is believed that the correlation is observed here because the emphasis is on collapse, unlike previous studies that considered less non-linear response levels. Additionally, this study uses a large number of ground motions over an extremely large magnitude range, which makes it more likely that any dependence would be detected.

To estimate collapse capacity as a function of epsilon, magnitude, and distance, linear least-squares regression analysis is performed and summarized in Table 2. The distance has been removed from the regression equation after a hypothesis test using analysis of variance, which indicates that distance has no statistically significant explanatory power.

Two parameters of the fragility function in equation (18) are estimated using the regression analysis result as follows:

$$\hat{\lambda} = \hat{\beta}_0 + \hat{\beta}_1 \times \varepsilon + \hat{\beta}_2 \times m, \quad \hat{\zeta} = \hat{\sigma}, \quad (20)$$

where  $\hat{\beta}_0, \hat{\beta}_1$ , and  $\hat{\beta}_2$  are the estimated values of coefficients given in Table 2.

The probability of collapse given  $S_a = x$ ,  $M = m$ , and  $R = r$  is thus calculated as

$$P(\text{collapse}|x, m, r) = \Phi\left(\frac{\ln(x) - (\hat{\beta}_0 + \hat{\beta}_1 \times \varepsilon + \hat{\beta}_2 \times m)}{\hat{\sigma}}\right), \quad (21)$$

where  $\varepsilon$  is calculated using equation (19) given the values of  $M$  and  $R$ .

Probability of the Occurrence of the Damage Event Given the IM,  $M$ , and  $R$  and Probability of the Occurrence of the Damage Event Given the  $M$

Given the probability of collapse given  $S_a$ ,  $M$ , and  $R$ , the probability of the occurrence of the damage event given the  $S_a$ ,  $M$ , and  $R$  is computed using equation (8). To compute the probability of the occurrence of the damage event given the magnitude using equation (12), we need  $f_{IM|M,R}(im|m, r)$  and  $f_R(r)$ . We used the KEPRI01 attenuation relationship

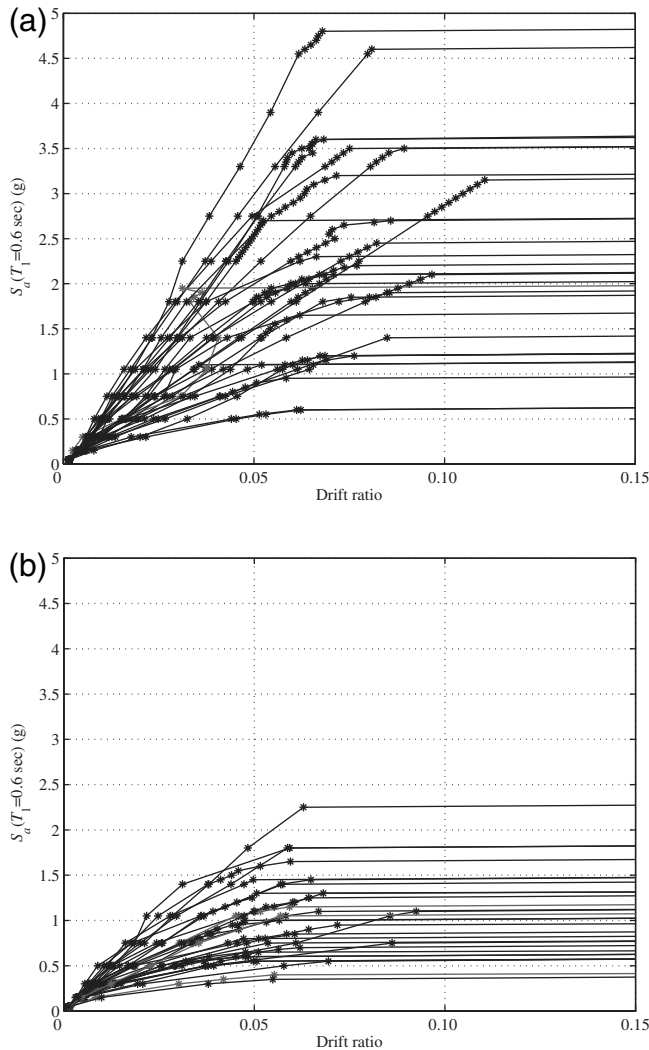


**Figure 9.** IDA curves for two bins of ground motions. (a)  $5 \leq M \leq 6$ ,  $0 \leq R \leq 50$ . (b)  $7 \leq M \leq 8$ ,  $50 \leq R \leq 100$ .

(KINS, 2003) to compute  $f_{IM|M,R}(im|m,r)$ , reflecting the characteristics of ground motions in Korea. Because we do not know the exact location of the epicenter and the collapsed structures from the 1613 earthquake, we set a distribution of distance from the epicenter as

$$f_R^1(r) = \frac{2}{r_u^2} r, \quad 0 \leq r \leq r_u, \quad (22)$$

where  $r_u$  is the upper limit of distance; this equation represents the distribution of distances' epicenter locations uniformly located within a circle of radius  $r_u$  around the structures. Note that a superscript 1 is added to distinguish this distribution from alternatives used later. The upper limit of distance ( $r_u$ ) is set to be 25 km, utilizing the information on the area of Seoul in 1613 (Im, 1985). Figure 11 shows the probability of the occurrence of the damage event given the magnitude and shows that an  $M$  7.7 earthquake has the highest probability of causing the given damage event.

### Posterior Distribution of Magnitude Given the Damage Event

In this example, we choose a uniform distribution of magnitude using equation (17), where  $m_l$  and  $m_u$  are set equal to 5 and 8, respectively, reflecting the range of magnitudes that are believed to be feasible in Korea and that could damage structures.

We compute the posterior probability distribution of magnitude given the damage event using equation (13). Figure 12 shows the prior distribution of magnitude as well as the posterior distribution given the damage event. We can compute the expected value and standard deviation of the posterior magnitude distribution as approximately 7.4 and 0.4, respectively. The posterior distribution is skewed to the left, as shown in Figure 12, because events greater than  $M$  8 have been truncated due to their believed infeasibility; the expected magnitude value would thus increase if the upper bound on feasible magnitudes were to be expanded.

### Discussion of Example Result

The earthquake damage record considered in this example is challenging because it provides only a so-called single data point (i.e., a single damage description). The magnitude estimate in this example is larger than previous research results obtained using empirical relationships between epicentral intensity and magnitude (e.g., 6.5 by Li, 1986). The estimated standard deviation is regarded as consistent with previous estimates, where typical values range from 0.4 to 0.5 (Sibol *et al.*, 1987; Casado *et al.*, 2000). However, these new results should not yet be interpreted as contradicting past magnitude estimates, because the results are dependent on several assumptions. The example serves to illustrate the methodology, but magnitude estimates will require refined input assumptions (e.g., analytic structural model parameters and prior probability distributions of magnitude and distance).

In the following sections, the proposed method will be extended to take the correlation of collapse capacity between structures, the effect of aging on structural response, and the site effects into account. Following that, we investigate the assumptions regarding the damage event, prior distributions of plausible magnitudes and distances, and the choice of attenuation relationship. These refinements will lead to more accurate magnitude estimates.

### Extension of the Proposed Method

#### Correlation of Collapse Capacity between Structures

The previous calculations assumed that collapses of structures were independent events (given ground-motion intensity, magnitude, and distance) with a fixed probability

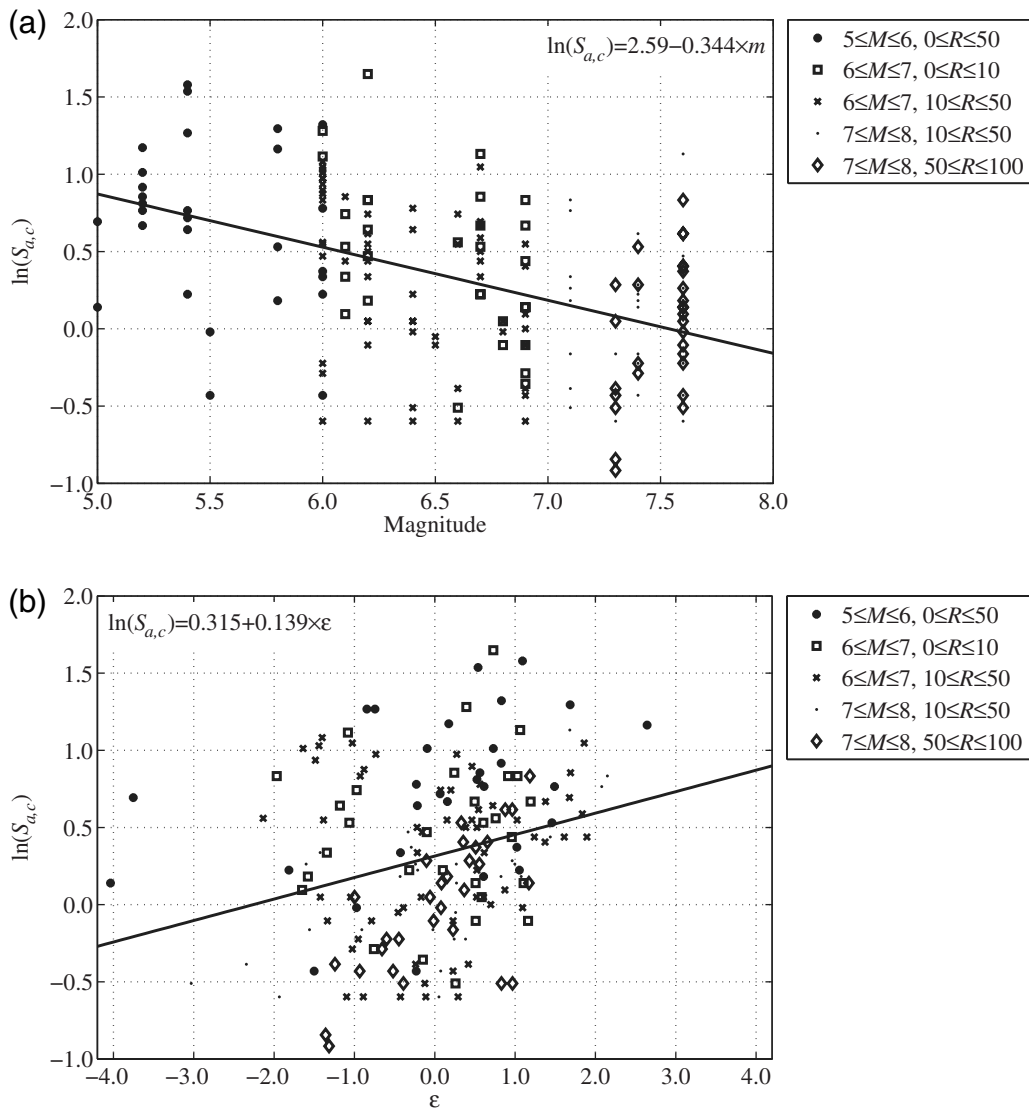


**Figure 10.** Scatter plots of magnitude and epsilon versus collapse capacity (i.e., the spectral accelerations at which each ground motion causes collapse). (a) Magnitude versus collapse capacity. (b) Epsilon versus collapse capacity.

of occurrence. However, there might be dependence in collapses caused by common workmanship or due to modeling errors that would be common to all structures. If the structural fragility function of a collapse state is defined with two parameters ( $\hat{\lambda}$  and  $\hat{\zeta}$ ) as in equation (18) and collapse ca-

capacity between any two structures is equicorrelated with a common correlation coefficient  $\rho$ , then the distribution of logarithmic collapse capacities of all  $n_t$  structures can be represented as an  $n_t$ -variate multivariate normal distribution with mean vector ( $\lambda$ ) and covariance matrix ( $\Sigma$ ) as

Table 2  
Regression Analysis Result

Regression Equation		$\ln(S_{a,c}) = \beta_0 + \beta_1 \times \epsilon + \beta_2 \times m$			
Coefficient	Estimated Value	Standard Error	t Value	p Value	
$\beta_0$	2.93	0.30	9.88	<0.001	
$\beta_1$	0.19	0.030	6.26	<0.001	
$\beta_2$	-0.40	0.045	-8.87	<0.001	
$N = 180$	$R^2 = 0.36$	$R_a^2 = 0.36$	$\hat{\sigma} = 0.43$	DOF = 177	

$N$  is the total number of data,  $R^2$  is the coefficient of determination,  $R_a^2$  is the adjusted  $R^2$ ,  $\hat{\sigma}$  is the standard deviation of the regression residuals, and DOF is the degree of freedom.

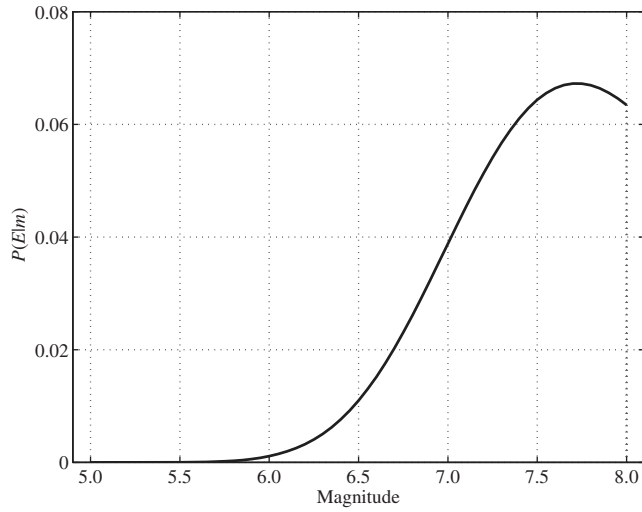


**Figure 11.** Probability of the occurrence of the damage event given the magnitude.

$$\ln \mathbf{S}_{a,c} \sim N(\boldsymbol{\lambda}, \boldsymbol{\Sigma}), \quad \text{where } \boldsymbol{\lambda} = [\hat{\lambda}_1, \dots, \hat{\lambda}_t]^T \quad \text{and} \quad (23)$$

$$\boldsymbol{\Sigma}_{i,j} = \begin{cases} \hat{\zeta}^2 & i = j \\ \rho \cdot \hat{\zeta}^2 & i \neq j \end{cases}$$

where  $\ln \mathbf{S}_{a,c}$  is a vector of correlated logarithmic collapse capacities for the structures,  $N()$  denotes the multivariate normal distribution, and boldface notation denotes matrices or vectors.

To compute the probability that  $n$  out of  $n_t$  structures collapse in an event, we must compute the probability that  $n$  out of  $n_t$  collapse capacities are less than some threshold. When the collapse capacities are independent, this probability can be computed using the binomial distribution. Here, where they are not independent, a Monte Carlo simulation must be used.

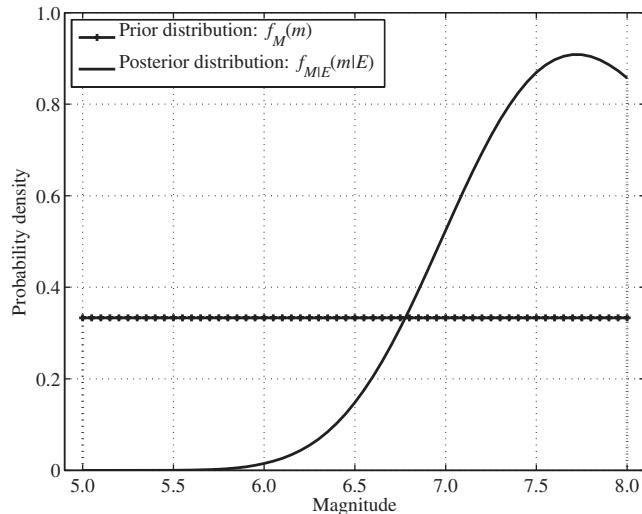


**Figure 12.** Posterior probability distribution of magnitude given the damage event with prior distribution of magnitude.

Using Monte Carlo simulation, one can repeatedly generate vectors of collapse capacity having the distribution specified in equation (23). The probability of occurrence of the damage event can then be computed as

$$P(E|IM = im, M = m, R = r) = P(l \leq N \leq u | im, m, r) = \frac{\text{number of simulations where } l \leq N \leq u}{\text{total number of simulations}}. \quad (24)$$

Figure 13a,b show the probability of the occurrence of the damage event and the posterior probability distribution of magnitude, respectively, using Monte Carlo simulation with different correlation values. The binomial distribution result is also shown to verify that it corresponds to the case of uncorrelated capacities. Figure 13a shows that when correlation is high, the considered damage event can be caused by a wider range of ground-motion intensity values. As correlation increases, structures tend to behave similarly, which means that the probability that all structures are either collapsed or noncollapsed increases.

As correlation increases, the expected value of magnitude increases while its standard deviation decreases. These tendencies are somewhat dependent on the parameter values of the damage event and lower and upper limits of magnitude but are generally consistent for the range of realistic parameter values.

#### The Effect of Aging on Structural Response

There are uncertainties in parameter values and numerical models for the construction of structural fragility functions because they are chosen based on the test results of the experimental model that is well constructed with good workmanship and tested not long after the construction. Thus, its seismic performance might be better than real structures.

Choi and Seo (2002) considered aging deterioration by assuming that the remaining capacity of a wooden house decreased linearly with time, based on empirical studies of earthquake damage to Japanese wooden structures

$$\alpha = 1 - \frac{t}{T}, \quad (25)$$

where  $\alpha$  is the remaining capacity ratio and  $T$  is the maximum service life of the house.

In this study, the remaining capacity ratio is implemented in the backbone curve as depicted in Figure 14, where the yield strength and yield displacement are proportional to the remaining capacity ratio while the stiffness remains the same. With this parameterization, it can be shown that the median collapse capacity of equation (20) becomes

$$\hat{\lambda} = \hat{\beta}_0 + \hat{\beta}_1 \times \varepsilon + \hat{\beta}_2 \times m + \ln(a), \quad (26)$$

where  $\hat{\beta}_0, \hat{\beta}_1,$  and  $\hat{\beta}_2$  are identical to the previous estimates;  $a$  is a value of the remaining capacity ratio  $\alpha$ .

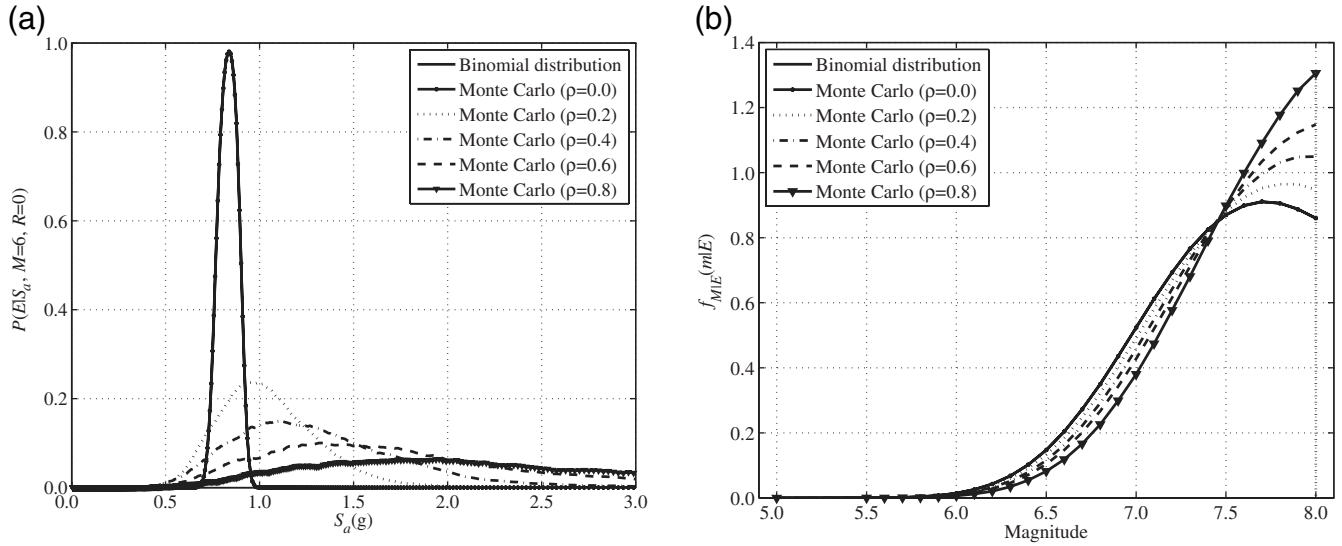


**Figure 13.** Comparison of results between using binomial distribution and Monte Carlo simulation for different correlation coefficients ( $\rho$ ). (a) Probability of the occurrence of the damage event given the spectral acceleration, magnitude, and distance. (b) Posterior probability distribution of magnitude given the damage event.

Then, the probability of collapse given  $S_a = x$ ,  $M = m$ ,  $R = r$ , and  $\alpha = a$  is calculated as follows:

$$P(\text{DM} = \text{collapse}|x, m, r, a) = \Phi\left(\frac{\ln(x) - [\hat{\beta}_0 + \hat{\beta}_1 \times \varepsilon + \hat{\beta}_2 \times m + \ln(a)]}{\hat{\sigma}}\right). \quad (27)$$

Given the probability of collapse given values of  $S_a$ ,  $M$ ,  $R$ , and  $\alpha$ , one can compute the probability of the occurrence of the damage event using either the binomial distribution or the Monte Carlo simulation. In the case of using binomial distribution, the probability of collapse given  $S_a = x$ ,  $M = m$ , and  $R = r$  is first computed using the total probability theorem:

$$P(\text{DM} = \text{collapse}|x, m, r) = \int P(\text{DM} = \text{collapse}|x, m, r, a) \times f_\alpha(a) da, \quad (28)$$

where  $f_\alpha(a)$  is the probability density function of the remaining capacity ratio (which is assumed to be uniform between 0.1 and 1 in this case). Given the probability of collapse, one can compute the probability of the occurrence of the damage event using equation (8) as in the example. In the case of using the Monte Carlo simulation, the remaining capacity ratio is randomly generated for each structure and then used to modify the simulated collapse capacities.

The expected values of magnitude obtained using the binomial distribution and the Monte Carlo approach (with  $\rho = 0$ ) are 6.4 and 6.5, respectively. The reason that the two results slightly differ can be explained as follows. With the binomial distribution, the aging effect is taken into account in the computation of the probability of the collapse as in equation (28) and then used for all structures. On the other hand, the Monte Carlo approach generates a unique remaining capacity ratio for each structure. The Monte Carlo approach more closely represents reality but also takes more computation time. With either computation approach, this aging effect modification dramatically lowers the estimated expected value of magnitude because the few older houses with lower capacities collapse more easily; thus, a smaller magnitude earthquake can cause the observed level of damage to the city.

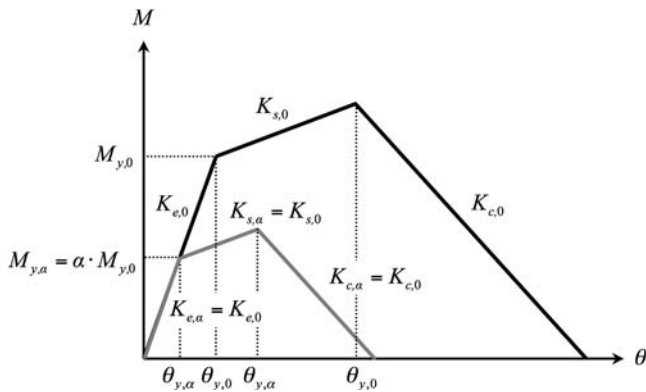


**Figure 14.** Effect of remaining capacity ratio on the structural elements' backbone curve. Parameters with the subscript  $\alpha$  are updated ones with the value of the remaining capacity ratio  $\alpha$ ; parameters with the subscript 0 represent the original value at the initial state.

### Site Effects

Earthquake ground motions and the resulting structural damage vary depending on the geologic and soil conditions

of the site where the structure is located. Site effects can be either probabilistically or deterministically taken into account. Using the probabilistic approach, we include the probability distribution of the ground-motion intensity at a site given the ground-motion intensity, magnitude, and distance in equation (12) as follows:

$$\begin{aligned}
P(E|m) &= \iiint P(E|im_{\text{site}}, m, r) \\
&\times f_{IM_{\text{site}}|IM,M,R}(im_{\text{site}}|im, m, r) \\
&\times f_{IM|M,R}(im|m, r) \times f_R(r) \dim_{\text{site}} \dim dr,
\end{aligned} \tag{29}$$

where  $im_{\text{site}}$  is the ground-motion intensity at a site and  $im$  is the ground-motion intensity at bedrock (unlike previously, where the soil condition was not stated).

The probability distribution of the ground-motion intensity at a site given the ground-motion intensity at bedrock, magnitude, and distance can be obtained by performing site response analysis (e.g., Bazzurro and Cornell [2004]).

Using an approximate deterministic approach, we simply modify equation (12) to include a site amplification factor (site coefficient), which is the ratio of the ground-motion intensity at a site to the ground-motion intensity at bedrock, as follows:

$$\begin{aligned}
P(E|m) &= \iint P(E|a_f \times im, m, r) \times f_{IM|M,R}(im|m, r) \\
&\times f_R(r) \dim dr,
\end{aligned} \tag{30}$$

where  $a_f$  is the site amplification factor at a site. The site amplification factor may be obtained in various ways, but it typically comes from site-specific studies.

In this study, the site effect is deterministically taken into account using the site amplification factor for simple implementation. The site where the damaged structure was located is assumed to be classified as National Earthquake Hazards Reduction Program (NEHRP) site class C (Building Seismic Safety Council [BSSC], 2001). It is recognized that site amplification factors are dependent on a base acceleration level (Borcherdt, 2002), but due to limited data in this case, the site amplification factor is set to a constant 1.3 based on the evaluation of site-specific seismic amplification characteristics in the plains of Seoul (Sun *et al.*, 2005).

Using this site amplification factor, the expected value and standard deviation of magnitude are found to be 6.3 and 0.5, respectively, when considering aging effects. This expected value is approximately 0.1 less than the case without considering site effects because smaller magnitudes now cause stronger ground motions and thus more collapses.

### The Effects of Other Parameter Values on the Magnitude Estimate

In this section, the effects of assumptions regarding the damage event, the prior distributions of plausible magnitudes

and distances, and the choice of attenuation relationship on the magnitude estimate are investigated. Studies of the structural system parameters are excluded because this has been done elsewhere (e.g., Ibarra [2003]). For comparison purposes, the remaining capacity ratio is assumed to have a uniform distribution between 0.1 and 1, collapses are assumed to be independent events, and no site effect is assumed.

### Damage Event

The damage event is defined with two parameters: the number of collapsed structures and the total number of structures. These values can be determined based on historical information but also on incorporated subjective judgments that should be investigated. First, the assumed number of collapsed buildings was varied from 1 to 2250, and the resulting expected value and standard deviation of estimated magnitude is shown in Figure 15. The expected value increases with the increment of the number of collapsed buildings; however, its variation is not linear. The standard deviation decreases with increasing number of collapses because the posterior distribution is truncated on the right due to an upper limit on the magnitude of plausible earthquakes.

Second, the effect of the range of the assumed number of collapsed buildings is investigated by computing posterior magnitude distributions when assuming a range of collapses with a lower bound of 1 and an upper bound ranging between 1 and 2250. As shown in Figure 16, the expected value and the standard deviation increase as this range increases but somewhat stabilize on the right side of the figure.

Third, the effect of total number of buildings is investigated by varying the assumed total number of buildings from 4500 to 450 and 45. As shown in Figure 17, the effect on the magnitude estimate is negligible as long as the ratio of collapsed buildings is held constant.

### Prior Distributions of Magnitude and Distance

In this section, alternative prior distributions of magnitude and distance are considered to investigate their effects on the estimated posterior magnitude.

To combine the previous research results on the estimation of the magnitude of the historical Korean event, we define an alternative magnitude distribution  $f_M^2(m)$  as follows:

$$f_M^2(m) = \frac{c}{m\zeta\sqrt{2\pi}} \exp\left(\frac{-(\ln m - \lambda)^2}{2\zeta^2}\right), \quad m_l \leq m \leq m_u, \tag{31}$$

where  $c$  is a normalizing constant and is equal to 0.954 with  $m_l = 5$ ,  $m_u = 8$ ,  $\lambda = 1.754$ , and  $\zeta = 0.086$ . This is a truncated lognormal distribution with parameters  $\lambda$  and  $\zeta$  that are estimated using the median estimated magnitude value of 5.8 obtained by other researchers (Table 1) and 0.5 that is a typical value for standard deviation. It should be noted that if one uses previous research to establish this prior distribution,

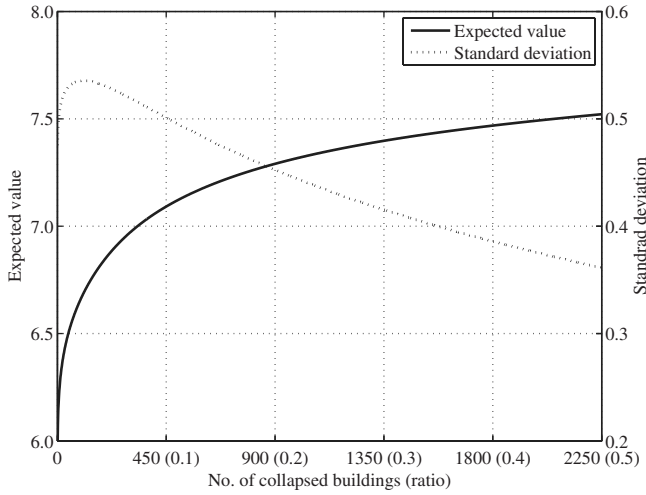


**Figure 15.** Expected value and standard deviation of magnitude as a function of the number of collapsed buildings.

care should be taken not to double count any information by using it in both the prior distribution and magnitude estimation procedure described here.

As another alternative, we choose a magnitude distribution following the doubly truncated Gutenberg–Richter relationship (Cosentino *et al.*, 1977):

$$f_M^3(m) = \frac{2.303 \times b \times 10^{-b(m-m_l)}}{1 - 10^{-b(m_u-m_l)}}, \quad m_l \leq m \leq m_u, \quad (32)$$

where  $m_l = 5$ ,  $m_u = 8$ , and  $b = 0.6$ . The coefficient  $b$  is chosen to represent the seismicity of Korea, based on the results by Lee and Kim (2000).

Assuming that both the site and epicenter are both uniformly distributed inside a circle of radius  $r_u$  (Kendall and Moran, 1963), we obtain an alternative distance distribution  $f_R^2(r)$  as follows:

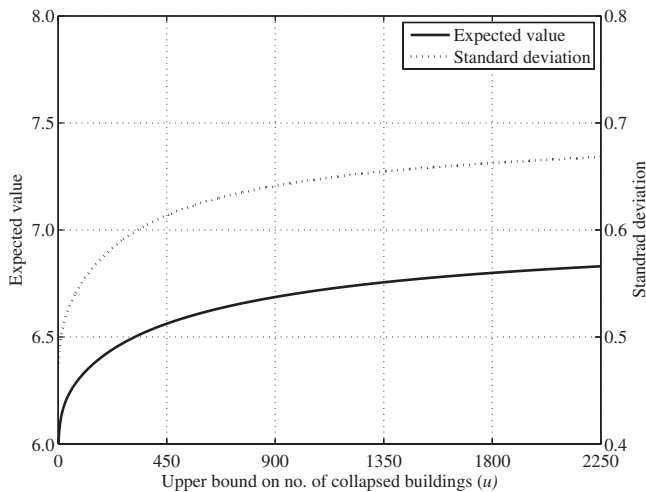


**Figure 16.** Expected value and standard deviation of magnitude given a range of collapsed buildings between 1 and  $u$ , where the upper bound  $u$  is varied on the  $x$  axis.

$$f_R^2(r) = \frac{8}{\pi r_u} (\theta \sin^2 \theta \cos \theta - \sin \theta \cos^2 \theta + \theta \cos^3 \theta), \quad (33)$$

$$0 \leq r \leq 2r_u,$$

where  $r_u = 12.5$  km and  $\theta = \cos^{-1}(\frac{r}{2r_u})$ .

Similarly, assuming that the site and epicenter are uniformly distributed in concentric circles (Fairthorne, 1964), we set  $f_R^3(r)$  as follows:

$$f_R^3(r) = \begin{cases} 2r/r_b^2 & 0 \leq r \leq r_b - r_a \\ \frac{r}{\pi} \left( \frac{2\alpha - \sin 2\alpha}{r_b^2} + \frac{2\beta - \sin 2\beta}{r_a^2} \right) & r_b - r_a \leq r \leq r_b + r_a \end{cases}, \quad (34)$$

where  $r_a = 5$  km,  $r_b = 20$  km,  $\alpha = \cos^{-1}(\frac{r^2 - r_b^2 + r_a^2}{2r_a r})$ , and  $\beta = \cos^{-1}(\frac{r^2 + r_b^2 - r_a^2}{2r_b r})$ . The values of the radii of circles in equations (33) and (34) are determined based on data on the area of Seoul in 1613 (Im, 1985). The alternative prior distributions of magnitude and distance are plotted in Figure 18a,b, respectively.

The expected value and standard deviation of magnitude associated with the various combinations of prior distributions are listed in Table 3. The expected values range from 5.9 to 6.4; standard deviations range from 0.4 to 0.5. Referencing Figure 18, one can see that the mean posterior magnitude decreases when the mean prior magnitude is lower. Loosely, the calculation shows that if small magnitude events are relatively more frequent, then it becomes more likely that a smaller magnitude caused the historically described damage. A similar trend is seen with standard deviations: if the standard deviation of the prior magnitude distribution decreases (i.e., the distribution is narrower), then the standard deviation of the posterior magnitude distribution will also decrease.

Rather than choosing a single pair of distributions as correct, one can also assume that the true distribution is unknown and incorporate this additional uncertainty using the total representation theorem (Ditlevsen, 1981)

$$\mu_{M|E} = E[\mu_{M|E,M^i,R^j}],$$

$$\sigma_{M|E} = \sqrt{E[\sigma_{M|E,M^i,R^j}^2] + \sigma^2[\mu_{M|E,M^i,R^j}]}, \quad 1 \leq i, j \leq 3, \quad (35)$$

where  $\mu_{M|E,M^i,R^j}$  and  $\sigma_{M|E,M^i,R^j}$  are the expected value and standard deviation computed with given  $f_M^i(m)$  and  $f_R^j(r)$ , respectively. Assuming that all of the aforementioned distributions have an equal probability of being correct, the resulting expected value and standard deviation are 6.1 and 0.5, respectively.

#### Attenuation Relationship

There is no other Korean attenuation relationship that provides the needed standard deviation of spectral accelera-

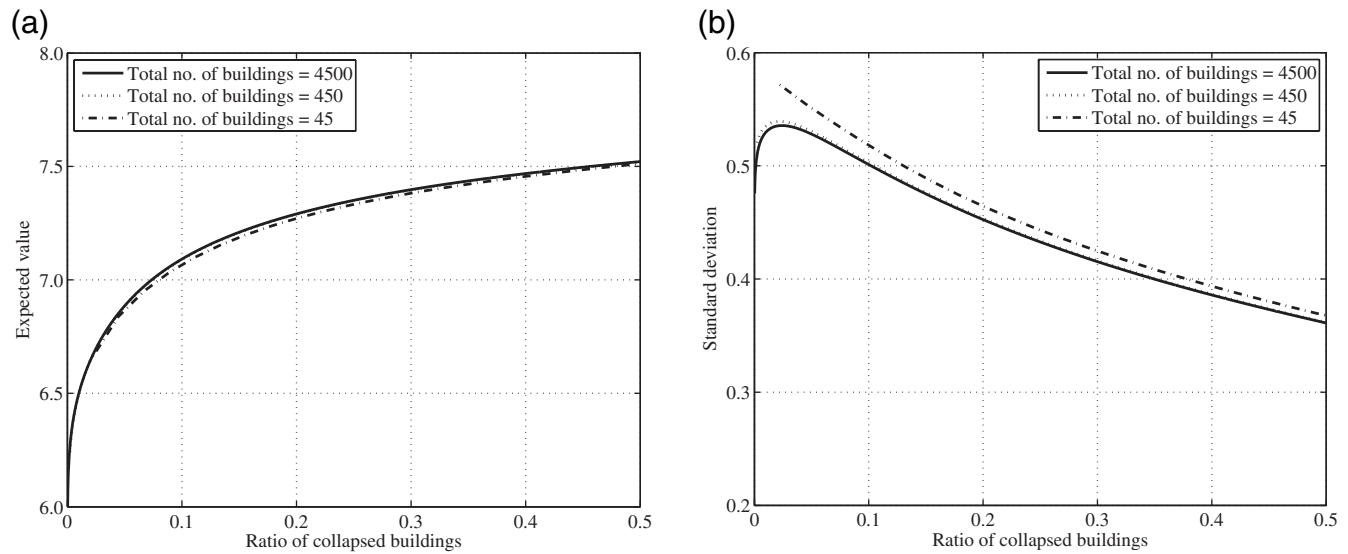


**Figure 17.** Expected value and standard deviation with a different total number of buildings. (a) Expected value. (b) Standard deviation.

tion, so fictitious values of standard deviation are used with the KEPRI01 attenuation relationship to perform a sensitivity analysis. When the standard deviation is cut in half, the expected value and standard deviation of magnitude are computed as 6.4 and 0.3, respectively. The reduction in the standard deviation of magnitude relative to the basic case is dramatic, which supports the intuitive idea that uncertainty in the magnitude estimate is primarily due to the large variability in ground-motion intensity associated with a given magnitude and distance.

The aforesaid sensitivity analyses suggest that while the estimated magnitude for this example varies with varying assumed input parameters, the differences are not great over the range of realistic parameter values. The ability to perform sensitivity analyses of this type is one advantage of the proposed method.

### Conclusion

A probabilistic method for estimating the magnitude of a historical damaging earthquake was described. In the proposed method, a qualitative description of structural damage in historical documents is transformed into a probabilistic damage event, and the posterior probabilistic distribution of magnitude given the damage event is computed using a structural fragility function, an attenuation equation, and prior distributions of magnitude and distance, by applying the total probability theorem and Bayes' theorem.

As a validation example, the magnitude of the 1994 Northridge earthquake was estimated. Given observations of damage to RC frame buildings and HAZUS fragility functions for that building class, the proposed method produced magnitude estimates that were very close to the known true

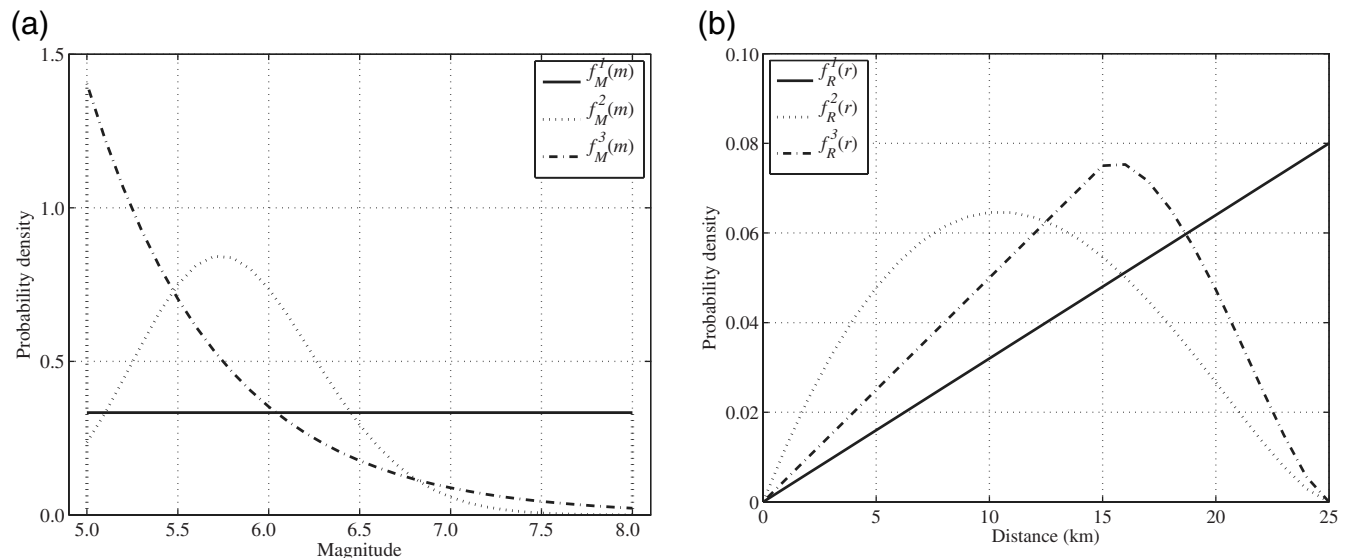


**Figure 18.** (a) Three choices for the prior distribution of magnitude. (b) Three choices for the prior distribution of distance.

Table 3

Expected Value and Standard Deviation (in Parentheses) of Magnitude with Respect to Prior Distributions of Magnitude and Distance

	$f_k^1(r)$	$f_k^2(r)$	$f_k^3(r)$
$f_M^1(m)$	6.4 (0.5)	6.3 (0.5)	6.3 (0.5)
$f_M^2(m)$	6.1 (0.4)	6.0 (0.4)	6.0 (0.4)
$f_M^3(m)$	6.1 (0.5)	5.9 (0.5)	6.0 (0.5)

magnitude of that event. As an application example, the magnitude of a historical Korean earthquake that occurred in 1613 was then estimated. The basic method was then extended to account for correlation of collapse capacity between structures, the effect of aging on structural capacity, and site effects. The effects of parameter values of the damage event, prior distributions of magnitude and distance, and the attenuation relationship on the magnitude estimate were also investigated.

The benefits of the proposed method are summarized as follows: first, it avoids the weaknesses of widely used traditional procedures. It does not use a traditional intensity scale such as MMI, which is considered an ambiguous characterization of structural damage. It is adaptable to various quantities of information, even being applicable to single point data as shown in the example. Second, it is a probabilistic procedure that can explicitly incorporate various sources of uncertainty. Uncertainty in the magnitude estimate can be quantified and propagation of uncertainty can be performed. The uncertainty can be potentially reduced by, for example, using a more sophisticated numerical model or a refined attenuation relationship. Third, it is a modular procedure and thus is easily extended to take into account other issues, such as correlation of collapse capacity between structures, without changing the basic framework. Fourth, by virtue of Bayes' theorem, it can incorporate subjective judgments and utilize previous research results with prior distributions of magnitude and distance (although information should not be double counted by utilizing information about the damage event to determine the prior distribution of magnitude).

The sensitivity analysis performed as part of the example calculation suggested that while the estimated magnitude was affected by varying the distributions of feasible magnitudes and distances, the differences are not great over the range of realistic parameter values. Aging effects did have a large effect on the estimate, suggesting that a representative numerical model is critical to the analysis. The uncertainty of the magnitude estimate was greatly affected by the uncertainty of the ground-motion attenuation relationship, suggesting that uncertainty in ground-motion attenuation is a dominant contributor to uncertainty in magnitude estimates. Reducing this uncertainty would thus be helpful, although it is practically difficult. The ability to perform sensitivity analyses of this type is one advantage of the proposed method. The proposed framework provides opportunities to continue improving magnitude estimates of historical earth-

quakes by refining individual analysis steps and evaluating the results of sensitivity analyses.

## Data and Resources

The image of the earthquake damage record was obtained from <http://silok.history.go.kr/> (last accessed on 1 March 2007).

## Acknowledgments

This work was partly supported by the Korea Research Foundation Grant funded by the Korean Government (MOEHRD) (KRF-2006-352-D00183), the fund of the Ministry of Science and Technology of Korea through the Korea Institute of Nuclear Safety (KINS) and the Korea Electric Power Research Institute (KEPRI), and the Korea Ministry of Construction and Transportation (MOCT) through the Korea Construction Engineering Development Collaboratory Program Management Center (KOCED PMC) at Seoul National University. We are very grateful to Walter J. Silva of Pacific Engineering and Analysis for his valuable comments on the selection and modification of ground motions.

## References

- Abrahamson, N. A., and W. J. Silva (1997). Empirical response spectral attenuation relations for shallow crustal earthquakes, *Seism. Res. Lett.* **68**, 94–127.
- Ambraseys, N. (1985). Intensity-attenuation and magnitude-intensity relationships for northwest European earthquakes, *Earthq. Eng. Struct. Dyn.* **13**, 733–778.
- Applied Technology Council (ATC) (1985). *Earthquake Damage Evaluation Data for California, ATC-13*, Applied Technology Council, Redwood City, California.
- Baker, J. W., and C. A. Cornell (2006). Spectral shape, epsilon and record selection, *Earthq. Eng. Struct. Dyn.* **35**, 1077–1095.
- Basoz, N., and A. S. Kiremidjian (1997). Evaluation of bridge damage data from the Loma Prieta and Northridge, CA earthquakes, John A. Blume Earthquake Engineering Center Technical Report No. 127 (also published as Technical Report No. MCEER-98-004).
- Bazzurro, P., and C. A. Cornell (1994). Seismic hazard analysis of nonlinear structures. I: methodology, *J. Struct. Eng.* **120**, 3325–3344.
- Bazzurro, P., and C. A. Cornell (2004). Ground-motion amplification in nonlinear soil sites with uncertain properties, *Bull. Seismol. Soc. Am.* **94**, 2090–2019.
- Benjamin, J. R., and C. A. Cornell (1970). *Probability, Statistics, and Decision for Civil Engineers*, McGraw-Hill, New York, 684 pp.
- Borcherdt, R. D. (2002). Empirical evidence for acceleration-dependent amplification factors, *Bull. Seismol. Soc. Am.* **92**, 761–782.
- Building Seismic Safety Council (BSSC) (2001). NEHRP recommended provisions for seismic regulations for new buildings and other structures, part 1: provisions, Federal Emergency Management Agency Report No. FEMA 368, 2000 Edition.
- Casado, C. L., S. Molina, J. J. Giner, and J. Delgado (2000). Magnitude-intensity relationships in the Ibero-Magrebhian region, *Nat. Hazards* **22**, 271–297.
- Castelli, V., and G. Monachesi (1996). Problems of reliability in earthquake parameters determination from historical records, *Ann. Geofis.* **39**, 1029–1040.
- Choi, I. K., and J. M. Seo (2002). Estimation of historical earthquake intensities and intensity-PGA relationship for wooden house damages, *Nucl. Eng. Des.* **212**, 165–182.
- Chu, K. S., and J. M. Lee (1999). Evaluation and collective arrangement of historical damaging earthquakes for the suggestion of new Korean

- seismic map, National Institute for Disaster Prevention Report No. 99-13, 180 pp. (in Korean).
- Cosentino, P., V. Ficara, and D. Luzio (1977). Truncated exponential frequency-magnitude relationship in the earthquake statistics, *Bull. Seismol. Soc. Am.* **67**, 1615–1623.
- Ditlevsen, O. (1981). *Uncertainty Modeling with Applications to Multi-dimensional Civil Engineering Systems*, McGraw-Hill, New York, 412 pp.
- Fairthorne, D. (1964). The distance between random points in two concentric circles, *Biometrika* **51**, 275–277.
- Federal Emergency Management Agency (FEMA) (2003). *HAZUS-MH MR-1 Technical Manual*, Federal Emergency Management Agency, Washington, D.C.
- Gutenberg, B., and C. F. Richter (1956). Earthquake magnitude, intensity, energy, and acceleration, *Bull. Seismol. Soc. Am.* **46**, 105–145.
- Ibarra, L. F. (2003). Global collapse of frames structures under seismic excitations, *Ph.D. Thesis*, Stanford University.
- Iervolino, I., and C. A. Cornell (2005). Record selection for nonlinear seismic analysis of structures, *Earthq. Spectra* **21**, 685–713.
- Im, D. S. (1985). *The Capital Origin and Developmental Process of Seoul*, *Ph.D. thesis*, Seoul National University (in Korean).
- Karim, K. R., and F. Yamazaki (2001) Effect of earthquake ground motions on fragility curves of highway bridge piers based on numerical simulation, *Earthq. Eng. Struct. Dyn.* **30**, 1839–1856.
- Kendall, M. G., and P. A. P. Moran (1963). *Geometrical Probability*, Griffin's Statistical Monographs and Courses, no. 10, Hafner Publishing Company, New York, 41–42.
- Kim, D. U. (1994). The city and architecture of Seoul during the late Choson period, *Korea J.* **34**, 54–68.
- Kim, J. K., and H. Ryu (2003). Seismic test of a full-scale model of a five-storey stone pagoda, *Earthq. Eng. Struct. Dyn.* **32**, 731–750.
- Kircher, C. A., A. Nassar, O. Kustu, and W. Holmes (1997). Development of building damage functions for earthquake loss estimation, *Earthq. Spectra* **13**, 663–682.
- Korea Institute of Nuclear Safety (KINS) (2003). Development of technology and background for seismic safety evaluation, KINS Final Report No. KINS/GR-255, 1433 pp. (in Korean).
- Korea Ministry of Construction and Transportation (KMOCT) (1997). *Research on Seismic Design Code (II)*, Korea Ministry of Construction and Transportation, Seoul, Korea (in Korean).
- Kyujanggak Institute for Korea Studies at Seoul National University (1996). *Hogu Chongsu* (Complete Register of Households), Seoul National University, Seoul, 10347 pp. (in Korean and Chinese).
- Lee, K. (1998). Historical earthquake data of Korea, *J. Korea Geophys. Soc.* **1**, 3–22 (in Korean).
- Lee, K., and J. K. Kim (2000). Seismic characteristics of tectonic provinces of the Korean peninsula, *J. Korea Geophys. Soc.* **3**, 91–98 (in Korean).
- Li, Y. C. (1986). *Korean Earthquake Catalogue (2 AD–1983)*, Seismological Press, Beijing, China, 69 pp.
- McGuire, R. K., W. J. Silva, and C. J. Costantino (2001). Technical basis for revision of regulatory guidance on design ground motions: hazard- and risk-consistent ground motion spectra guidelines, U.S. Nuclear Regulatory Commission Report No. NUREG/CR-6728.
- McKenna, F., and G. L. Fenves (2001). *The OpenSees Command Language Manual*, Pacific Earthquake Engineering Research (PEER) Center, University of California, Berkeley, also available at <http://opensees.berkeley.edu> (last accessed 1 March 2007).
- Moroni, A., G. Monachesi, and D. Albarello (1996). Intensity assessment from documentary data: criteria and procedures in the daily practice of seismologists, *Ann. Geofis.* **39**, 969–979.
- Muramatu, I. (1969). Relation between the distribution of seismic intensity and the earthquake magnitude, *Sci. Rep. Fac. Ed. Gifu Univ. Nat. Sci.* **4**, 168–176 (in Japanese).
- Musson, R. M. W. (1996). Determination of parameters for historical British earthquakes, *Ann. Geofis.* **39**, 1041–1047.
- Nuttl, O. W., and R. B. Herrmann (1978). State-of-the-art for assessing earthquake hazards in the United States, in *Credible Earthquakes for the Central United States*, Miscellaneous Paper S-73-1, Report 12, U.S. Army Engineer Waterways Experiment Station, Vicksburg, Mississippi, 99 pp.
- Nuttl, O. W., G. A. Bollinger, and D. W. Griffiths (1979). On the relation between modified Mercalli intensity and body-wave magnitude, *Bull. Seismol. Soc. Am.* **69**, 893–909.
- Office of Emergency Services (OES) (1995). *The Northridge Earthquake of January 17, 1994: Report of Data Collection and Analysis, Part A: Damage and Inventory Data*, prepared by EQE International, Incorporated, and the Geographic Information Systems Group of the Governor's Office of Emergency Services for the Governor's Office of Emergency Services of the State of California.
- Park, Y.-J., and A. H.-S. Ang (1985). Mechanistic seismic damage model for reinforced concrete, *J. Struct. Eng.* **111**, no. 4, 722–739.
- Ryu, H., Y. C. Huh, and J. K. Kim (2006). The evaluation of seismic performance of Korean traditional wood frame buildings with thatched roof, *Proceedings of the 8th U.S. National Conference on Earthquake Engineering*, Paper No. 491, 18–22 April 2006, San Francisco, California.
- Seo, J. M., I. K. Choi, and J. R. Lee (1999). Experimental study on the aseismic capacity of a wooden house using shaking table, *Earthq. Eng. Struct. Dyn.* **28**, 1143–1162.
- Seoul Development Institute (SDI) (1999). Earthquake response system models for the Seoul metropolitan government, 653 pp. (in Korean).
- Shome, N., C. A. Cornell, P. Bazzurro, and J. E. Carballo (1998). Earthquakes, records and nonlinear responses, *Earthq. Spectra* **14**, 469–500.
- Sibol, M. S., G. A. Bollinger, and J. B. Birch (1987). Estimation of magnitudes in central and eastern North America using intensity and felt area, *Bull. Seismol. Soc. Am.* **77**, 1635–1654.
- Silva, W. J., and K. Lee (1987). WES RASCAL code for synthesizing earthquake ground motions, state-of-the-art for assessing earthquake hazards in the United States, U.S. Army Corps of Engineers Waterways Experiment Station Report No. 24, Miscellaneous Paper S-73-1, 120 pp.
- Singhal, A., and A. S. Kiremidjian (1998). Bayesian updating of fragilities with application to RC frames, *J. Struct. Eng.* **124**, 922–929.
- Sun, C. K., D. S. Yang, and C. K. Chung (2005). Evaluation of site-specific seismic amplification characteristics in plains of Seoul metropolitan area, *J. Earthq. Eng. Soc. Korea* **9**, 29–42 (in Korean).
- Toppozada, T. R. (1975). Earthquake magnitude as a function of intensity data in California and western Nevada, *Bull. Seismol. Soc. Am.* **65**, 1223–1238.
- Vamvatsikos, D., and C. A. Cornell (2002). Incremental dynamic analysis, *Earthq. Eng. Struct. Dyn.* **31**, 491–514.

Department of Civil and Environmental Engineering  
Stanford University  
Stanford, California 94305  
dynaryu@gmail.com  
(H.R., J.W.B.)

Department of Civil and Environmental Engineering  
Seoul National University  
Kwanak-ku, Seoul 151-742, Korea  
(J.K.K.)